

Attenuation of Insulin-Evoked Responses in Brain Networks Controlling Appetite and Reward in Insulin Resistance

The Cerebral Basis for Impaired Control of Food Intake in Metabolic Syndrome?

Karen Anthony,¹ Laurence J. Reed,² Joel T. Dunn,³ Emma Bingham,¹ David Hopkins,¹ Paul K. Marsden,³ and Stephanie A. Amiel¹

The rising prevalence of obesity and type 2 diabetes is a global challenge. A possible mechanism linking insulin resistance and weight gain would be attenuation of insulin-evoked responses in brain areas relevant to eating in systemic insulin resistance. We measured brain glucose metabolism, using [¹⁸F]fluorodeoxyglucose positron emission tomography, in seven insulin-sensitive (homeostasis model assessment of insulin resistance [HOMA-IR] = 1.3) and seven insulin-resistant (HOMA-IR = 6.3) men, during suppression of endogenous insulin by somatostatin, with and without an insulin infusion that elevated insulin to 24.6 ± 5.2 and 23.2 ± 5.8 mU/l ($P = 0.76$), concentrations similar to fasting levels of the resistant subjects and approximately threefold above those of the insulin-sensitive subjects. Insulin-evoked change in global cerebral metabolic rate for glucose was reduced in insulin resistance (+7 vs. +17.4%, $P = 0.033$). Insulin was associated with increased metabolism in ventral striatum and prefrontal cortex and with decreased metabolism in right amygdala/hippocampus and cerebellar vermis ($P < 0.001$), relative to global brain. Insulin's effect was less in ventral striatum and prefrontal cortex in the insulin-resistant subjects (mean \pm SD for right ventral striatum 3.2 ± 3.9 vs. 7.7 ± 1.7 , $P = 0.017$). We conclude that brain insulin resistance exists in peripheral insulin resistance, especially in regions subserving appetite and reward. Diminishing the link be-

tween control of food intake and energy balance may contribute to development of obesity in insulin resistance. *Diabetes* 55:2986–2992, 2006

The explosion in rates of obesity, type 2 diabetes, and cardiovascular disease and the associated metabolic abnormalities have been termed the “diabesity pandemic” (1). It is of paramount importance to understand the etiology of the cluster of pathologies that comprise the increased risk. Insulin resistance is a linking component and central adiposity is a defining feature (2–4). Lifestyle factors, particularly excess consumption of palatable food and reduced exercise, have been incontrovertibly associated with insulin resistance (5,6), yet are notoriously resistant to change. Despite the obvious importance of brain networks in control of behavior, including food seeking (7,8), possible alterations in the functioning of these networks in insulin resistance have not been examined. This may be because of lack of knowledge of the role of insulin in central nervous system function.

Insulin transporters, receptors, and insulin-dependent GLUT4 transporters are widespread in animal and human brain (9,10), GLUT4 being predominantly neuronal and responsive to glucose and insulin (11). These data allow for an important central role for insulin, either to stimulate glucose metabolism directly or to function as a neurotransmitter, stimulating neuronal glucose uptake indirectly. There is evidence for a range of central roles for insulin, unrelated to peripheral metabolic effects, including on feeding behavior, sensory processing, and cognitive function (12–15). Although human studies comparing basal and high circulating insulin concentrations have not demonstrated any differences in brain glucose metabolism (16,17), recent data from our group have shown an insulin-sensitive element to brain glucose metabolism in humans, responsive to changes in peripheral insulin, which may be maximal at low insulin concentrations (18). The demonstration of insulin-responsive human brain glucose metabolism allows investigation of the hypothesis that brain insulin resistance exists in people with peripheral insulin resistance. If so, this will be an important tool and target in investigating and treating links between insulin resistance

From the ¹Diabetes Research Group, King's College London School of Medicine, King's College, London, U.K.; the ²Division of Psychological Medicine, Institute of Psychiatry, King's College, London, U.K.; and ³The PET Imaging Centre, King's College London School of Medicine, King's College, London, U.K.

Address correspondence and reprint requests to Prof. Stephanie A. Amiel, Medical School Building, King's College London School of Medicine, King's College Hospital Campus, Bessemer Road, London, SE5 9PJ, U.K. E-mail: stephanie.amiel@kcl.ac.uk

Received for publication 21 March 2006 and accepted in revised form 11 August 2006.

Additional information for this article can be found in an online appendix at <http://diabetes.diabetesjournals.org>.

CMRglc, cerebral metabolic rate for glucose; FDG, [¹⁸F]fluorodeoxyglucose; HOMA-IR, homeostasis model assessment of insulin resistance; PET, positron emission tomography; SPM, Statistical Parametric Mapping.

DOI: 10.2337/db06-0376

© 2006 by the American Diabetes Association.

The costs of publication of this article were defrayed in part by the payment of page charges. This article must therefore be hereby marked “advertisement” in accordance with 18 U.S.C. Section 1734 solely to indicate this fact.

and appetite control and also between insulin resistance and cerebral function (19,20).

Investigation of the regional pattern of insulin sensitivity may provide clues to the role of insulin within cerebral networks. To investigate the hypotheses that brain insulin resistance exists in people with systemic insulin resistance and specifically affects networks involved in appetite and food intake, we have measured insulin-evoked global and regional brain glucose uptake and metabolism in insulin-sensitive and insulin-resistant healthy volunteers using [^{18}F]fluorodeoxyglucose (FDG)-positron emission tomography (PET).

RESEARCH DESIGN AND METHODS

Fourteen healthy male volunteers (aged 49 ± 9.6 years), characterized for insulin sensitivity, were recruited. The study was restricted to men to decrease additional endocrine sources of variability and because of radiation exposure. Insulin sensitivity was estimated using the homeostasis model assessment of insulin resistance (HOMA-IR) calculation, based on fasting glucose and insulin concentrations ($\text{insulin } [\mu\text{U/ml}] \times \text{glucose } [\text{mmol/l}]/22.5$) (21). $\text{HOMA-IR} \geq 2.77$ defined insulin resistance. This encompasses $\sim 20\%$ of the population and predicts highest risk of development of metabolic syndrome, being associated with increased prevalence of its features (22). Seven of our subjects were selected to be in this category and underwent an oral glucose tolerance test; none had diabetes, although two had impaired glucose tolerance according to World Health Organization criteria (23). The other seven subjects were selected to have HOMA-IR in the lowest two quintiles for a normal population, < 1.55 , as showing normal insulin sensitivity. These two quintiles do not differ from each other in terms of absence of markers of the metabolic syndrome. Data from five of the insulin-sensitive and two of the insulin-resistant subjects were included in a previous publication (18).

The protocol was approved by the research ethics committees of King's College Hospital and St. Thomas' Hospital NHS Trusts and ARSAC (Administration of Radioactive Substances Advisory Committee). Volunteers gave informed written consent before study.

Study protocol. Each volunteer underwent two FDG-PET studies, 3–8 weeks apart, in random order. Studies were performed in the morning after an overnight fast. An intravenous cannula for infusion of drugs and fluids was placed in an antecubital vein of the dominant arm using aseptic technique and skin anesthesia (1% lidocaine). After ensuring satisfactory collateral circulation, a second cannula was placed in the radial artery of the nondominant hand for arterial sampling. Somatostatin (Stilamin; Serono, Switzerland) was infused at $0.1 \text{ mg} \cdot \text{kg}^{-1} \cdot \text{min}^{-1}$ to suppress endogenous insulin secretion in all studies. During one scan, $0.3 \text{ mU} \cdot \text{kg}^{-1} \cdot \text{min}^{-1}$ regular insulin (Human Actrapid; Novo Nordisk, Denmark), diluted in a 4% saline solution of autologous blood, was infused. During the other, a control saline infusion was given. Arterial plasma glucose was measured at the bedside every 5 min. A variable-rate 20% glucose infusion (Fresenius Kabi, Warrington, U.K.) was used if necessary to maintain euglycemia.

Positron emission tomography. The volunteer was moved into the PET scanner (CTI ECAT 951R scanner, axial field view 10.8 cm, in-plane spatial resolution 6.5 mm; CTI/Siemens, Nashville, TN). The head was aligned axially to the orbitomeatal line and position maintained using a restraining strap. Scanning was performed with the volunteer's eyes closed to minimize effects of external sensory input. Scanning was started after 90 min of somatostatin infusion (with or without insulin) to allow achievement of steady-state glucose. A transmission scan was performed in the last 10 min, then a single dose of $\sim 150 \text{ MBq}$ FDG, made up to 10 ml with normal saline, was injected over 10 s, followed by 10 ml normal saline over 10 s. Dynamic scanning was performed over 90 min. Continuous arterial blood sampling to measure tracer levels was started 1 min before tracer injection, at 5 ml/min for 15 min then 2.5 ml/min for 15 min, the blood being drawn through an online radioactivity monitor (Allogg, Sweden). Every 5 min a 2-ml sample of arterial blood was drawn for measurement of plasma glucose and cross-calibration of the fluid analyzer data with a well counter, allowing an arterial plasma input function to be derived for each study.

Image data analysis. PET images were reconstructed by filtered back projection and smoothed to obtain a spatial resolution of 8.5 mm full-width at half-maximum both transaxially and axially. Reconstructed images were displayed in a $128 \times 128 \times 31$ voxel format. Each voxel measured $2 \times 2 \times 3.375 \text{ mm}$. Whole-brain cerebral metabolic rate of glucose (CMR_{glc}) was calculated in $\text{ml} \cdot 100 \text{ g}^{-1} \cdot \text{min}^{-1}$ using the Patlak method (24). The average plasma glucose concentration is explicitly accounted for using this method; however, in order to eliminate any possible effects of variations in plasma

glucose concentration during data acquisition, CMR_{glc} was also calculated with an explicit correction for this. (Briefly, assuming Michaelis-Menten kinetics and constant CMR_{glc}, a corrected constant clearance rate can be determined if the plasma FDG concentration is multiplied by a factor inversely proportional to the plasma glucose at each time point. This corrected clearance rate can then be used to calculate CMR_{glc} in the normal way. Both methods are described in the online appendix, which can be found at <http://diabetes.diabetesjournals.org>.)

For regional analysis, FDG uptake images created by summation of the images acquired 20–60 min after injection were analyzed using Statistical Parametric Mapping (SPM) Version 2 (SPM2; <http://www.fil.ion.ucl.ac.uk/spm>), developed at the Wellcome Department of Cognitive Neurology (London), running in Matlab 6 (Mathworks, Sherborn, MA). SPM involves registration of each data set onto a common "standard" brain, elimination of global effects as a covariate of no interest, and then comparing activity in each voxel statistically, using an appropriate correction for multiple comparisons. In this way, SPM identifies brain regions where insulin is having a greater or lesser effect, relative to the global effect. Each participant's scans were realigned and transformed into Montreal Neurological Institute (MNI) standard stereotactic space using affine and nonlinear deformation to the template provided in SPM2 to allow interindividual averaging and comparison. Smoothing was performed on all scans using an isotropic Gaussian Kernel of 12 mm to allow for differences in gyral anatomy between individuals and to increase signal-to-noise ratios (25,26). The effect of interindividual variance in scans from differing injected doses was removed by using proportional scaling. Global FDG uptake was arbitrarily normalized to 50, and the threshold for inclusion of voxels for statistical analysis was 0.8. Comparisons of condition and group-by-condition interactions were made by definition of the appropriate linear contrasts within SPM2. Clusters of voxels showing a peak T score > 3.93 , cluster size $k > 100$, were considered significant. The high T score minimizes risk of finding false-positives and uses a statistical threshold of $P < 0.001$.

Further to investigate brain regional involvement, individual regional CMR_{glc} in clusters (or volumes of interest) exhibiting suprathreshold behavior on the above analysis were calculated. Data were compared using SPSS 13 (SPSS, Woking, U.K.) and Excel 97. For these comparisons of regions identified as different by the SPM analysis, differences between the two groups (given as insulin-evoked response and calculated by subtracting the data from the somatostatin + saline from the somatostatin + insulin data) were considered significant when $P < 0.05$. Data are given as means \pm SD, unless otherwise stated.

Biochemical analyses. Plasma glucose was measured using a glucose oxidase analyser (Yellow Springs Instruments, Yellow Springs, OH); insulin by radioimmunoassay (Diagnostics Systems Laboratories, London), with 50% cross-reactivity for proinsulin and split products; and C-peptide by radioimmunoassay (Diagnostic Systems Laboratories). Data are presented as means \pm SD. Differences were considered significant when $P < 0.05$ (Excel 97).

RESULTS

As shown in Table 1, the groups were significantly different in fasting glucose and insulin concentrations and HOMA-IR, all parameters being higher in the insulin-resistant group. The groups were not significantly different in BMI.

Plasma insulin and glucose. Fasting insulin concentrations were 7.09 ± 2.60 and $8.30 \pm 3.72 \text{ mU/l}$ on the 2 days in the insulin-sensitive and 22.62 ± 11.43 and $22.12 \pm 14.59 \text{ mU/l}$ in the insulin-resistant volunteers. Somatostatin suppressed endogenous insulin production, as measured by C-peptide concentration, in both groups in both studies (Fig. 1A). There were no significant differences between insulin concentrations between the groups, in either the saline-infused studies (2.57 ± 1.83 and $1.23 \pm 2.89 \text{ mU/l}$, $P = 0.33$) or in somatostatin plus insulin infusion (24.6 ± 5.2 vs. $23.2 \pm 5.8 \text{ mU/l}$, $P = 0.76$), the latter being significantly higher than in the saline control ($P < 0.0001$) and equivalent to the basal insulin of the resistant group (Fig. 1B). Thus, the insulin infusion maintained plasma insulin around fasting levels in the insulin-resistant subjects and brought about an approximately threefold increase over fasting levels in the insulin-sensitive subjects.

TABLE 1
Subject metabolic characteristics at assessment

	Insulin sensitive	Insulin resistant	<i>P</i>
<i>n</i>	7	7	
Fasting glucose (mmol/l)	4.8 (4.2–5.8)	5.7 (5.1–6.6)	0.014
Fasting insulin (mU/l)	6.3 (5.0–8.5)	25.1 (11.6–41.8)	0.005
HOMA-IR	1.3 (0.92–1.58)	6.3 (2.94–9.5)	0.026
BMI (kg/m ²)	26.9 (23.9–30)	28.4 (23.7–35.3)	0.41

Data are median (range).

Arterial plasma glucose concentrations are shown in Fig. 1C. For the insulin-sensitive subjects, mean plasma glucose during the 90-min scanning period was 5.6 ± 0.6 mmol/l with somatostatin alone and 5.2 ± 0.4 mmol/l with somatostatin plus insulin ($P = 0.097$). For the insulin-resistant subjects, mean plasma glucose was 6.5 ± 0.6 mmol/l during somatostatin alone and 5.7 ± 0.4 mmol/l during somatostatin plus insulin ($P = 0.008$), but the magnitude of the rise in plasma glucose during the study

was not different between the two groups ($P = 0.168$). The difference between the somatostatin alone and the somatostatin with insulin studies was significant only during the last 30 min of scanning.

Infusion rates of glucose during the scans were higher with insulin infusion (3.31 ± 1.39 mg · kg⁻¹ · min⁻¹ in the insulin-sensitive and 2.11 ± 1.14 mg · kg⁻¹ · min⁻¹ in the insulin-resistant subjects) than without (0.21 ± 0.25 and 0.02 ± 0.02 mg · kg⁻¹ · min⁻¹) but not significantly different

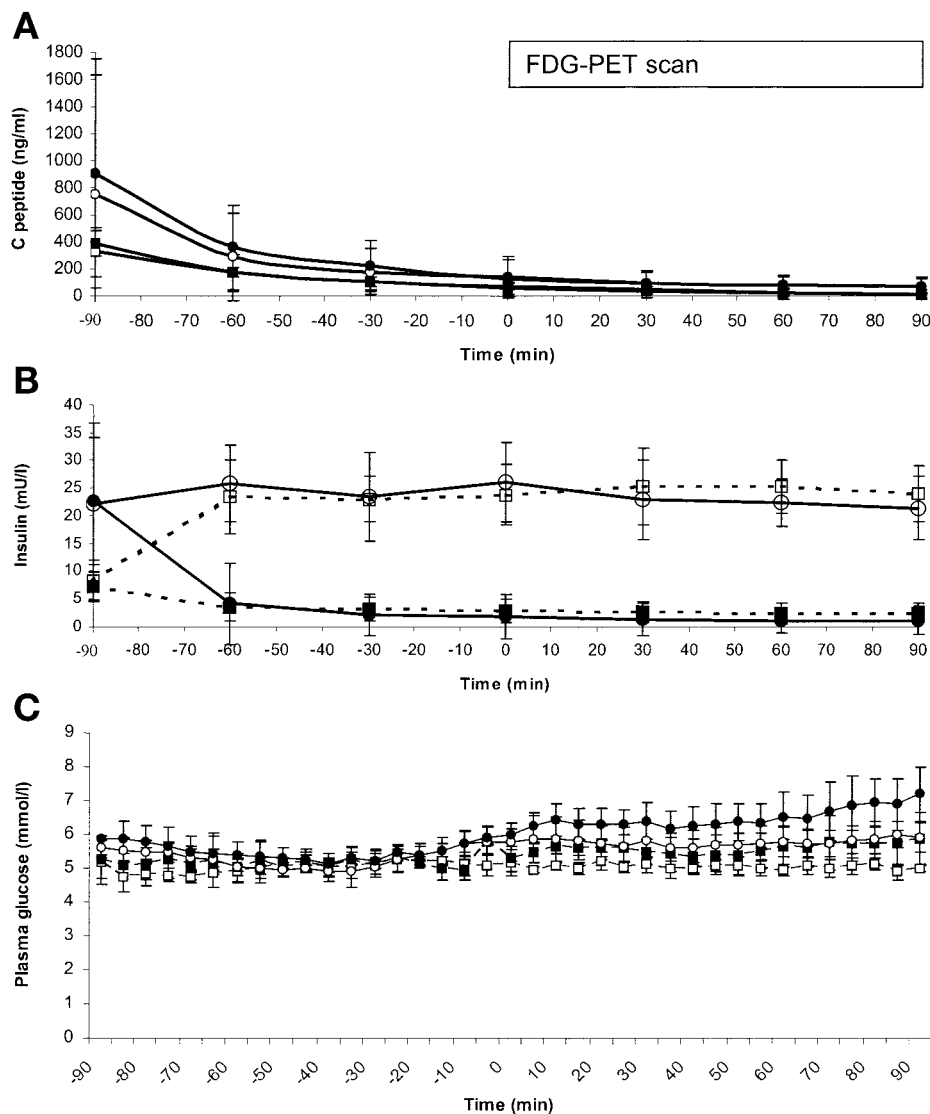


FIG. 1. Metabolic responses to somatostatin and insulin. C-peptide responses during somatostatin infusion (A), showing equivalent suppression in insulin-sensitive (squares) or insulin-resistant (circles) groups and in insulin-replaced (open symbols) and saline control subjects (closed symbols). Insulin infusion raised circulating insulin levels significantly over saline-infused studies in both groups (B). Plasma glucose (C) rose with somatostatin infusion; the highest increases appeared in the saline-infused studies in the insulin-resistant group, reaching significance after 60 min.

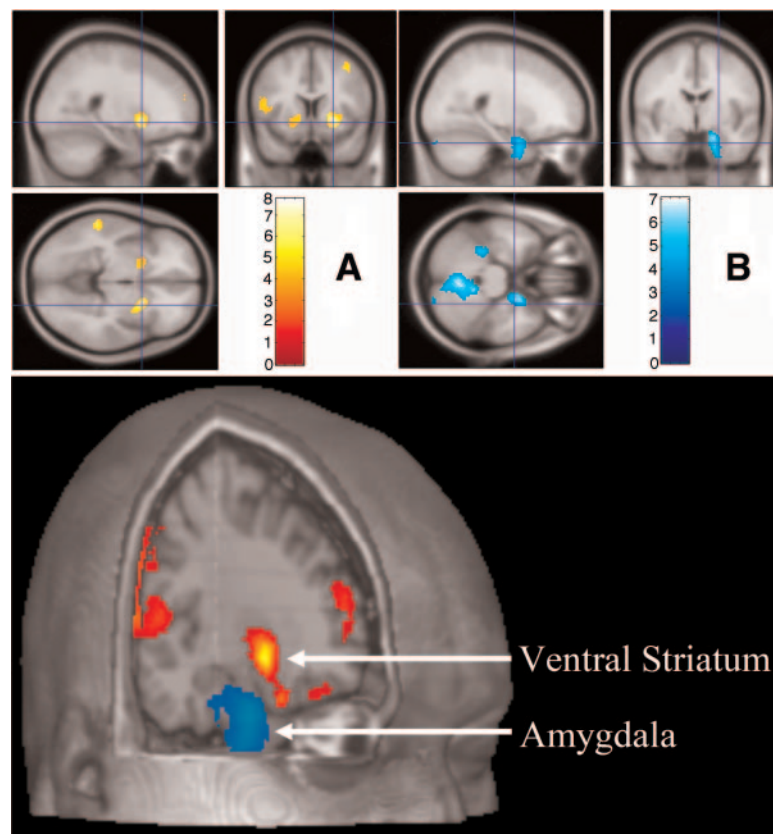


FIG. 2. Insulin-evoked cerebral responses. *A* (top left): Sagittal, coronal, and axial sections from SPM showing relative increases in cerebral metabolism in bilateral ventral striatum, using data from all subjects. *B* (top right): Sagittal, coronal, and axial sections from SPM showing relative decreases in cerebral metabolism in right amygdala and cerebellar vermis. *Bottom panel:* Rendered three-dimensional sections showing close apposition of relative increase in metabolism in right ventral striatum (yellow) with right amygdala decreases. Cluster statistics for regions shown are presented in Table 2.

between groups in either state ($P = 0.12$ and 0.071 respectively).

Whole-brain glucose metabolism. Low-dose insulin infusion was associated with an elevation in global brain cerebral metabolic rate for glucose (CMR_{glc}) in both groups. The effect was significantly less ($P = 0.033$, group versus condition interaction) in the insulin-resistant group, in which CMR_{glc} rose by only 7% (23.97 ± 2.88 to $25.8 \pm 3.34 \mu\text{mol} \cdot 100 \text{g}^{-1} \cdot \text{min}^{-1}$, $P = 0.028$) compared with 17.4% (20.91 ± 2.66 to $25.3 \pm 2.4 \mu\text{mol} \cdot 100 \text{g}^{-1} \cdot \text{min}^{-1}$, $P = 0.0025$) in the insulin-sensitive subjects. Recalculating CMR_{glc} values incorporating the correction for variation in plasma glucose during data acquisition described above resulted in changes of $<5\%$ in any of the CMR_{glc} values with no changes in the statistical relationships.

Relative regional brain FDG uptake. Investigation of regional cerebral glucose uptake using statistical parametric mapping showed that for both groups, the effect of insulin to increase glucose uptake was maximal in the ventral striatum bilaterally and prefrontal cortex including insula ($P < 0.001$, cluster size >100 voxels), regions involved in reward and feeding responses (8). The cluster statistics are shown in Table 2, detailing the size of each brain region identified in number of voxels (k); the cluster statistic and the Talairach coordinates giving the anatomical location of the cluster in the coronal (x), axial (y) and sagittal (z) planes. Insulin was associated with reduced regional glucose uptake, relative to global, in midline cerebellar vermis and right amygdala ($P < 0.001$), with left

amygdala showing a similar response at lower statistical threshold ($P < 0.005$; not shown). The amygdala has a crucial role in mediating fear and vigilance (27).

To more fully investigate regional cerebral involvement in response to insulin, a lower statistical threshold of $P < 0.05$ was used for SPM analysis. This showed relative increases in response to insulin in an extensive region of prefrontal and temporal cortex, including bilateral insular cortices; anterior cingulate cortex; and retrosplenial cortex. Furthermore, this analysis also showed decreases in a single contiguous cluster spanning left and right amygdala/hippocampal regions, midline cerebellar vermis, and lateral cerebellar cortices bilaterally (Fig. 2).

Quantitative analysis of the effect of insulin on regional brain glucose metabolism. Repeated-measures ANOVA was performed on the quantified effect of insulin replacement on CMR_{glc} in the clusters of interest, right prefrontal cortex, right ventral striatum, right amygdala, and cerebellar vermis (and contralateral coordinates). Quantitative CMR_{glc} for these clusters is given in Table 3. Bilateral ventral striatum, cerebellum, and prefrontal cortex showed significant effects of insulin (condition $P < 0.001$) with right ventral striatum and prefrontal cortex showing a significant group-by-condition interaction effect (Fig. 3). Post hoc t tests confirmed that the effect of insulin in this network of regions was reduced in the insulin-resistant group. The quantitative changes in the amygdala were attenuated, as compared with ventral striatum, and compatible with the SPM data. On the right side, there were no significant effects of subject group, insulin infu-

TABLE 2
Cluster statistics for regions with greater or lesser insulin response from SPM analysis

Brain region	Cluster size (<i>k</i>)	T statistic	MNI coordinates, showing anatomical location in three plains in standard space		
			<i>x</i>	<i>y</i>	<i>z</i>
Regions showing significant increase in insulin effect relative to global effect					
Right ventral striatum	329	7.98	22	10	-4
Left ventral striatum	109	4.81	-14	8	-2
Left insula	281	5.01	-42	20	8
Left infero-temporal cortex	446	7.51	-62	-30	-22
Right temporo-parietal junction	393	5.70	60	-24	26
Regions showing significant decrease in insulin effect relative to global effect					
Middle cerebellar vermis	550	6.59	22	2	-26
Right amygdala	1,860	6.92	6	-52	-34

sion, or the interaction between the two, while on the left side, there was an effect of insulin (condition $P = 0.033$) in the insulin-sensitive group (Fig. 3). This was not found in the insulin-resistant group in the post hoc analysis, although there was no significant effect of group in the ANOVA.

DISCUSSION

This study provides the first evidence for insulin resistance in brain glucose metabolism in human systemic insulin resistance. Using FDG-PET measures of CMRglc in the presence of somatostatin, with and without low-dose insulin infusion, we have demonstrated that the insulin-sensitive component of brain glucose metabolism comprises 15–20% of the resting brain glucose metabolic rate in insulin-sensitive individuals. However, in insulin-resistant individuals, insulin-evoked increases in whole-brain CMRglc are less than half of this for the same insulin increment. It is of crucial significance that these effects are most marked in brain regions involved in appetite control and motivational behaviors.

No previous human studies have measured brain glucose metabolism in insulin resistance. Our protocol used suppression of endogenous insulin and infusion of low circulating insulin and measurement of brain glucose uptake with labeled [^{18}F]fluorodeoxyglucose to examine the effects of insulin on brain glucose metabolism. The low concentrations of insulin used allowed us to find the insulin effect, presumably maximal at relatively low insulin doses. This effect was missed by earlier studies comparing physiological with supraphysiological insulin concentra-

tions (16,17). In the present protocol, insulin infusion maintained circulating insulin at the fasting level of the insulin-resistant subjects and brought the circulating insulin level in the insulin-sensitive subjects approximately threefold above their fasting level. The insulin concentrations were, however, matched between the two groups in both the insulin-withdrawn and the insulin-replaced states, allowing a comparison of the change in brain glucose metabolism between the two insulin concentrations achieved. One other study has investigated the effect of low-dose insulin on brain glucose uptake and did not find an effect (28). This was a magnetic resonance spectroscopy study, conducted at hyperglycemia (16.7 mmol/l), which may have rendered it less sensitive. Fluorodeoxyglucose, as used in the present protocol, is given in tracer amounts; it is taken up into cells via glucose transporters and undergoes initial phosphorylation as native glucose but is not metabolized further. Phosphorylated FDG accumulates in cells, creating a large signal, which is independent of cerebral blood flow and for which validated methods for calculating overall glucose metabolic rate are available for use at physiological plasma glucose levels (29). The insulin-evoked responses in CMRglc may be a direct effect of insulin on cell metabolism, or most likely an indirect effect, with insulin acting to stimulate neuronal activation. In either event, the changes seen can be attributed to changes in neuronal metabolism, rather than any effect of insulin on vasculature, as FDG uptake is insensitive to alterations in cerebral perfusion (29).

Although somatostatin has effects other than suppression of insulin, there is no reason to believe these effects

TABLE 3
Quantified regional CMRglc (in $\mu\text{mol} \cdot 100 \text{ g}^{-1} \cdot \text{min}^{-1}$) means and SDs within groups and conditions, with analysis of effects (from repeated-measures ANOVA)

Region	Insulin sensitive		Insulin resistant		<i>P</i>		Group by condition
	Saline	Insulin	Saline	Insulin	Group	Condition	
Ventral striate (right)	27.18 ± 2.99	34.90 ± 4.07*	31.12 ± 6.31	34.35 ± 4.92	0.493	2.08E-05	0.017
Ventral striate (left)	29.24 ± 3.65	36.82 ± 3.65*	30.84 ± 6.40	35.76 ± 6.78*	0.923	2.44E-05	0.183
Cerebellum	18.44 ± 1.92	21.62 ± 2.05*	20.99 ± 3.37	22.47 ± 3.64	0.266	2.21E-04	0.082
Amygdal (right)	15.65 ± 2.87	18.13 ± 2.00	18.40 ± 2.23	17.13 ± 4.50	0.528	0.529	0.069
Amygdala (left)	17.65 ± 2.55	20.00 ± 0.96†	20.14 ± 3.73	21.09 ± 1.94	0.146	0.033	0.328
Prefrontal cortex	25.03 ± 3.08	33.61 ± 3.99*	27.70 ± 7.23	32.65 ± 6.03*	0.761	9.64E-07	0.031

Post-hoc analysis (saline vs. insulin, within-group paired *t* test): * $P < 0.01$; † $P < 0.05$.

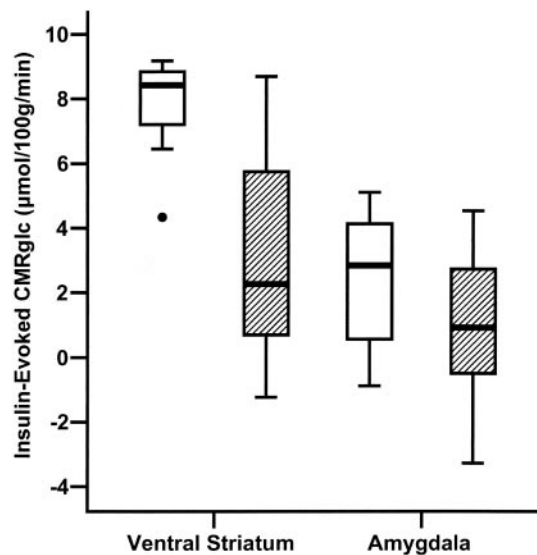


FIG. 3. Quantitative insulin-evoked cerebral responses in insulin-sensitive and insulin-resistant groups. The plot shows the distribution of insulin-evoked quantitative CMRglc in right ventral striatum and amygdala of the insulin-resistant (▨) and insulin-sensitive (□) groups. The solid bars show the medians, the boxes show the first and third quartiles, and the T bars show the range. The insulin effect was significantly attenuated in insulin-resistant subjects in the ventral striatum but not in amygdala. The point shows an outlier, whose data are also included in the plot.

will have been different between the insulin-resistant and insulin-sensitive subjects. The somatostatin infusion did not abolish the peripheral insulin resistance of the insulin-resistant subjects, who showed a slightly greater drift in plasma glucose concentration, especially without insulin replacement. Ideally, all studies would have been carried out at the same glucose level, but giving exogenous glucose would have been a further variable, and we carried out three separate assessments to check that the differences in plasma glucose observed at the end of the scanning time had not influenced the calculations of CMRglc. Nevertheless, it would be useful to construct dose-response curves for a series of different concentrations of both glucose and insulin to define the magnitude of the insulin resistance effect.

Regional analysis of our data showed that the effect of insulin (expressed as the difference between the somatostatin + saline and somatostatin + insulin studies) on brain glucose metabolism, relative to global metabolism, is highly regionally selective. The SPM analysis, which corrects for global differences between groups, shows the most robust insulin-driven increases in relative glucose metabolism in bilateral ventral striatum and prefrontal cortex, including the insula. This network is involved in the integration of food-seeking behavior and food intake with hypothalamic energy balance control systems (8). The ventral striatum in particular mediates reward responses and has received intense interest in addictive disorders (30,31). A role for insulin in this region is highly relevant to food-seeking and feeding behaviors, implicating insulin in the reward sensations associated with eating, which themselves reflect the importance of food intake to survival. It is noteworthy that the NIRKO mouse, with disruption of neuronal insulin signaling by knock out of the neuronal insulin receptors, demonstrates enhanced feeding behavior, particularly in females (32).

Dysregulation of these regional responses in insulin

resistance may be very important in the etiology of insulin resistance in obesity. Obesity has been associated with reduced dopamine activity in ventral striatum in humans (20), as has drug addiction (33). Our data indicate a possible mechanism for a reduced link between adequate energy intake and control of eating in insulin-resistant individuals. The present novel demonstration of insulin responsiveness in the ventral striatum, which is reduced in people characterized by insulin resistance (not necessarily with obesity), suggests the possibility that these changes are intrinsic to insulin resistance and may contribute to the evolution of insulin resistance into obesity and metabolic syndrome. We hypothesize that people with insulin resistance will need to generate a higher circulating insulin in order to experience the reward sensations of eating.

Relative increases in insulin-evoked glucose metabolism were also seen in prefrontal and insular (gustatory) cortices. These regions have been identified as having abnormal activation on refeeding in obese subjects, as well as in obese people who had dieted back to normal body habitus, implying an abnormality of the brain's response to food in the obese, which is either poorly reversible or which may be causative (34). Our finding of reduced insulin-evoked brain glucose metabolic responses in insulin-resistant subjects who were not necessarily yet obese may be important in the propensity of insulin-resistant people to develop obesity. We may speculate that the involvement of reward-seeking behaviors in the insulin-responsive networks may contribute to difficulties in changing eating behaviors in insulin resistance.

The SPM analysis also indicated relative decreases in glucose metabolism with insulin in cerebellar vermis and right amygdala/hippocampus, left amygdala being involved at a lesser statistical threshold. The cerebellar vermis was identified in our previously published dataset (18), in which we had sought only decreases in relative insulin effect using an older version of SPM. These relative decreases in FDG uptake indicate relative reduction in neuronal activation in these brain areas with insulin, and the attenuated response in quantitative CMRglc is consistent with this. The amygdala is activated by fear, resulting in enhanced vigilance (27). Reductions in amygdala activity have been observed in euphoric drug responses (35). The cerebellar (limbic) vermis is known to be involved in mood regulation, and damage to this structure can result in a range of mood disturbances ranging from euphoria and disinhibition to emotional blunting (36,37). Matsuda et al. (38) have described reduced hypothalamic inactivation in response to glucose ingestion in obese people with high fasting insulin concentrations, which may be part of the same picture. We may speculate that the relative suppression of the regions by insulin seen in our study is consistent with the comfort associated with eating. Although in our data, the effect of insulin in the amygdala was not significantly affected by insulin resistance, a possible hypothesis is that the hyperinsulinemic response to eating seen in nondiabetic insulin-resistant individuals may create an exaggerated comfort sensation after food, again encouraging further eating.

In conclusion, our data show that the effect of low circulating levels of insulin is to stimulate cerebral metabolism within appetite and reward networks, focusing on the ventral striatum in the healthy human brain. For a given insulin concentration, this effect is reduced in insulin-resistant individuals, most markedly in the ventral striatum, consistent with an emerging picture of reduced

function within cerebral reward networks in those at risk of overeating and obesity. These data support an etiological model of progressive dysregulation of reward networks on repeated exposure to palatable foods in people with insulin resistance. If confirmed, they provide a rationale for development of potential new treatments directed against the rising tide of insulin resistance syndromes and obesity and a method by which to monitor their effects.

ACKNOWLEDGMENTS

This study was supported by a research grant from Diabetes UK. K.A. was a Clinical Research Training Fellow of the Diabetes Research and Wellness Foundation, U.K.

We thank our research nurses Andrew Pernet and Bula M. Wilson for their support of the studies and the chemists and radiographers of the PET Imaging Centre at St. Thomas' Hospital, London.

REFERENCES

- Zimmet P, Alberti KG, Shaw J: Global and societal implications of the diabetes epidemic. *Nature* 414:782–787, 2001
- Reaven G: Role of insulin resistance in human disease. *Diabetes* 37:1595–1607, 1988
- Executive Summary of the Third Report of the National Cholesterol Education Program (NCEP) Expert Panel on Detection, Evaluation, and Treatment of High Blood Cholesterol in Adults (Adult Treatment Panel III). *JAMA* 285:2486–2497, 2001
- Balkau B, Charles MA: Comment on the provisional report from the WHO consultation. European Group for the Study of Insulin Resistance (EGIR). *Diabet Med* 16:442–443, 1999
- Berthoud HR, Berthoud HR: Mind versus metabolism in the control of food intake and energy balance. *Physiol Behav* 81:781–93, 2004 Jul.
- Erlanson-Albertsson C: How palatable food disrupts appetite regulation. *Basic Clin Pharmacol Toxicol* 2:61–73, 2005
- Spiegel A, Nable E, Volkow N, Landis S, Li TK: Obesity on the brain. *Nat Neurosci* 8:552–553, 2005
- Kelley AE: Ventral striatal control of appetitive motivation: role in ingestive behavior and reward-related learning. *Neurosci Biobehav Rev* 27:765–776, 2004
- Hopkins DF, Williams G: Insulin receptors are widely distributed in human brain and bind human and porcine insulin with equal affinity. *Diabet Med* 14:1044–1050, 1997
- El Messari S, Ait-Ikhlef A, Ambroise DH, Penicaud L, Arluison M: Expression of insulin-responsive glucose transporter GLUT4 mRNA in the rat brain and spinal cord: an in situ hybridization study. *J Chem Neuroanat* 24:225–242, 2002
- Alquier T, Leloup C, Arnaud E, Magnan C, Penicaud L: Altered Glut4 mRNA levels in specific brain areas of hyperglycemic-hyperinsulinemic rats. *Neurosci Lett* 308:75–78, 2001
- Porte D Jr, Baskin DG, Schwartz MW: Leptin and insulin action in the central nervous system. *Nutr Rev* 60:S20–S29, 2002
- Rotte M, Baerecke C, Pottag G, Klose S, Kanneberg E, Heinze HJ, Lehnert H: Insulin affects the neuronal response in the medial temporal lobe in humans. *Neuroendocrinology* 81:49–55, 2005
- Kern W, Peters A, Fruehwald-Schultes B, Deininger F, Born J, Fehm HL: Improving influence of insulin on cognitive function in humans. *Neuroendocrinology* 74:270–280, 2001
- Craft S, Asthana A, Newcomer J, Wilkinson CW, Matos IT, Baker LD, Cherrier M, Lofgreen C, Latendresse S, Petrova A, Plymate S, Raskind M, Grimwood K, Veith RC: Enhancement of memory in Alzheimer disease with insulin and somatostatin but not glucose. *Arch Gen Psychiatry* 56:1135–1140, 1999
- Hasselbalch SG, Knudsen GM, Videbaek C, Pinborg LH, Schmidt JF, Holm S: No effect of insulin on glucose blood-brain barrier transport and cerebral metabolism in humans. *Diabetes* 48:1915–1921, 1999
- Cranston I, Marsden P, Matyka K, Evans M, Lomas J, Sonksen P: Regional differences in cerebral blood flow and glucose utilization in diabetic man: the effect of insulin. *J Cereb Blood Flow Metab* 18:130–140, 1998
- Bingham EM, Hopkins D, Smith D, Pernet A, Hallett W, Reed L: The role of insulin in human brain glucose metabolism: an ¹⁸F-fluoro-deoxyglucose positron emission tomography study. *Diabetes* 51:3384–3390, 2002
- Stolk RP, Breteler MMB, Ott A, Pols HAP, Lamberts SWJ, Grobbee DE, Hofman A: Insulin and cognitive function in an elderly population. *Diabetes Care* 20:792–795, 1997
- Kuusisto J, Koivisto K, Mykkanen L, Helkala EL, Vanhanen M, Hanninen T, Kesaniemi A, Riekkinen PJ, Laakso M: Association between features of the insulin resistance syndrome and Alzheimer's: cross-sectional population-based study. *BMJ* 315:1045–1050, 1997
- Matthews DR, Hosker JP, Rudenski AS, Naylor BA, Treacher DF, Turner RC: Homeostasis model assessment: insulin resistance and beta-cell function from fasting plasma glucose and insulin concentrations in man. *Diabetologia* 28:412–419, 1985
- Bonora E, Kiechl S, Willeit J, Oberhollenzer F, Egger G, Targher G: Prevalence of insulin resistance in metabolic disorders: the Bruneck Study. *Diabetes* 47:1643–1649, 1998
- Zimmet P, Alberti KG: Definition, diagnosis and classification of diabetes mellitus and its complications. Part 1: diagnosis and classification of diabetes mellitus provisional report of a WHO consultation. *Diabet Med* 15:539–553, 1998
- Patlak CS, Blasberg RG, Fenstermacher JD: Graphical evaluation of blood-to-brain transfer constants from multiple-time uptake data. *J Cereb Blood Flow Metab* 3:1–7, 1983
- Friston KJ, Ashburner J, Frith CD, Poline J-B, Heather JD, Frackowiak RSJ: Spatial registration and normalization of images. *Human Brain Mapping* 3:165–188, 1995
- Friston KJ, Holmes AP, Worsley KJ, Poline J-B, Frith CD, Frackowiak RSJ: Statistical parametric maps in functional imaging: a general linear approach. *Hum Brain Mapp* 2:189–210, 1995
- Davis M, Whalen PJ: The amygdala: vigilance and emotion. *Mol Psychiatry* 6:13–34, 2001
- Sequist ER, Damberg GS, Tkac I, Gruetter R: The effect of insulin on in vivo cerebral glucose concentrations and rates of glucose transport/metabolism in humans. *Diabetes* 50:2203–2209, 2001
- Chen K, Bandy D, Reiman E, Huang SC, Lawson M, Feng D, Yun LS, Palant A: Noninvasive quantification of the cerebral metabolic rate for glucose using positron emission tomography, 18F-fluoro-2-deoxyglucose, the Patlak method, and an image-derived input function. *J Cereb Blood Flow Metab* 18:716–723, 1998
- Wise RA: Brain reward circuitry: insights from unsensed incentives. *Neuron* 36:229–240, 2002
- Wang GJ, Volkow N, Logan J, Pappas NR, Wong CT, Zhu W, Netusil N, Fowler JS: Brain dopamine and obesity. *Lancet* 357:354–357, 2001
- Bruning JC, Gautam D, Burks DJ, Gillette J, Schubert M, Orban PC, Klein R, Krone W, Muller-Weiland D, Kahn CR: Role of brain insulin receptor in control of body weight and reproduction. *Science* 289:2122–2125, 2000
- Kalivas PW, Volkow ND: The neural basis of addiction: a pathology of motivation and choice. *Am J Psychiatry* 162:1403–1413, 2005
- Del Parigi A, Chen K, Salbe AD, Hill JO, Wing RR, Reiman EM, Tataranni PA: Persistence of abnormal neural responses to a meal in post obese individuals. *International J Obesity* 28:370–377, 2004
- Rauch SL, Shin LM, Wright CI: Neuroimaging studies of amygdala function in anxiety disorders. *Ann N Y Acad Sci* 985:389–410, 2003
- Breiter HC, Gollub RL, Weisskoff RM, Kennedy DN, Makris N, Berke JD, Goodman JM, Kantor HL, Gastfriend DR, Riorden JP, Mathew RT, Rosen BR, Hyman SE: Acute effects of cocaine on human brain activity and emotion. *Neuron* 19:591–611, 1997
- Schmahmann JD, Sherman JC: The cerebellar cognitive affective syndrome. *Brain* 121:561–579, 1998
- Matsuda M, Liu Y, Mahankali S, Pu Y, Mahankali A, Wang J, DeFronzo RA, Fox PT, Gao JH: Altered hypothalamic function in response to glucose ingestion in obese humans. *Diabetes* 48:1801–1806, 1999